cussion of this problem is premature.

*Work supported by the Deutsche Forschungsgemeinschaft.

[1]H. Kanazawa, Prog. Theor. Phys. 26, 851 (1961).
[2]R. H. Ritchie, Prog. Theor. Phys. 29, 607 (1963).
[3]A. J. Benett, Phys. Rev. B 1, 203 (1970).
[4]Ch. Heger and D. Wagner, Z. Phys. 244, 449 (1971).
[5]J. Harris, J. Phys. C 5, 1757 (1972).
[6]J. Heinrichs, Phys. Rev. B 7, 3487 (1973).
[7]D. E. Beck and V. Celli, Surf. Sci. 37, 48 (1973).
[8]P. J. Feibelman, Phys. Rev. B 9, 5077 (1974).
[9]A. D. Boardman, B. V. Paranjape, and R. Teshima, Surf. Sci. 49, 275 (1975).
[10]C. Kunz, Z. Phys. 196, 311 (1966).
[11]T. Kloos and H. Raether, Phys. Lett. 44A, 157 (1973).
[12]J. Langkowski, cited by H. Raether, in *Proceedings of the Fourth International Conference on Vacuum Ultraviolet Radiation Physics, Hamburg, 1974*, edited by E. E. Koch, R. Haensel, and C. Kunz (Pergamon, New York, 1974), p. 597.
[13]T. Kloos, Z. Phys. 265, 225 (1973).
[14]P. Schmüser, Z. Phys. 180, 105 (1964).
[15]C. B. Duke and U. Landman, Phys. Rev. B 8, 505 (1973).
[16]J. O. Porteus and N. W. Faith, Phys. Rev. B 12, 2097 (1975).
[17]C. B. Duke, L. Pietronero, J. O. Porteus, and J. F. Wendelken, Phys. Rev. B 12, 4059 (1975).
[18]R. Y. Koyama, N. V. Smith, and W. E. Spicer, Phys. Rev. B 8, 2426 (1973).
[19]J. Schilling, Z. Phys. B25, 61 (1976).

Spin-Flip Raman Echo in *n*-Type CdS

P. Hu, S. Geschwind, and T. M. Jedju
Bell Laboratories, Murray Hill, New Jersey 07974
(Received 12 October 1976)

We report on the first observation of a Raman echo, using spin-flip Raman scattering at 4905 Å of bound donors in CdS to create a coherent spin state. The free-induction decays associated with each pulse in the sequence of two $\pi/2$ pulses as well as the echo are probed by spin-flip Raman scattering at 4880 Å.

A powerful tool for studying the microscopic or irreversible phase memory time of any two-level system is the class of well-known spin[1] and photon echo experiments.[2] Since it has been demonstrated very early that coherent states can be prepared by stimulated Raman scattering or two-wave mixing,[3] it is to be concluded that an echo signal can be generated by either of these processes and is called a Raman echo.[4] However, while various other coherent phenomena involving two-photon process have recently been demonstrated,[5] we report here the first observation of a Raman echo.

Spontaneous[6] and stimulated[7] spin-flip scattering were first observed in InSb and later in CdS.[8,9] For two time-reversed states $|a\rangle$ and $|b\rangle$ [see Fig. 1(a)] split in a magnetic field along z by $\hbar\omega_{ba}$ and for cubic symmetry,[10] the effective spin-flip Hamiltonian $H_{sp}^{(2)}$ was first given by Yafet as[11-13]

$$H_{sp}^{(2)} = \tfrac{1}{2}\alpha\vec{\sigma}\cdot(\vec{E}_L \times \vec{E}_R) \times \exp[i(\omega_L - \omega_R)t - (\vec{k}_L - \vec{k}_R)\cdot\vec{r}] + \text{c.c}, \quad (1)$$

where $\vec{E}_L$ is the laser field and $\vec{E}_R$ the Raman field with angular frequencies ω_L, ω_R and wave vectors $\vec{k}_L, \vec{k}_R$, respectively; $\vec{\sigma}$ are the Pauli matrices; $\vec{r}$ is the position vector of the impurity in the crystal; and α is related to the spontaneous differential Raman cross section $d\sigma/d\Omega$ by[12] $d\sigma/d\Omega = 4|\alpha|^2(\omega_L + \omega_{ba})^3\omega_L/c^4$. α becomes very large when $\hbar\omega_L$ is near-resonant to an excited state, which is the exciton bound to a neutral donor in our case.[8] Since in Eq. (1), $\alpha(\vec{E}_L \times \vec{E}_R)\exp[i(\omega_L - \omega_R)t]$ acts as an effective resonant rf magnetic

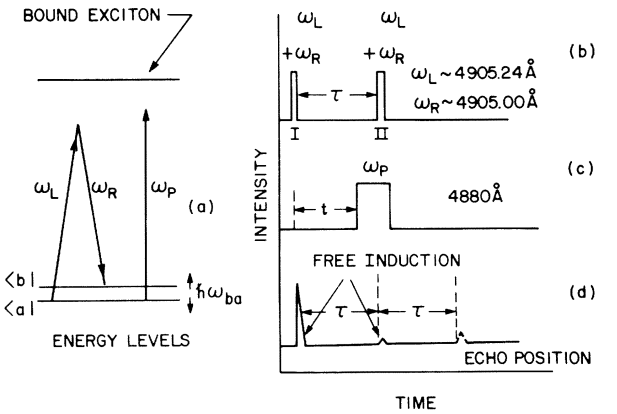

FIG. 1. (a) Energy levels in a Raman echo experiment. The excited state here is an exciton bound to a neutral donor. (b) The excitation pulse sequence of the dye laser. (c) The argon probe timing. (d) Expected behavior of 4880-Å Stokes free-induction and echo signals.

field with $\omega_L - \omega_R = \omega_{ba}$,[13] it generates a coherent transverse magnetization $\propto \frac{1}{2}\sigma_T$ which may be calculated using the standard magnetic resonance expressions and is given by

$$\sigma_T = \sin\theta \cos[(\vec{k}_L - \vec{k}_R)\cdot\vec{r}], \quad (2)$$

where θ is the "tipping angle" given by

$$\theta = \tfrac{1}{2}\hbar^{-1}(c^2/\omega_L^2)(d\sigma/d\Omega)_{4905}^{1/2}(E_R E_L)(\Delta t). \quad (3)$$

Δt is the duration of the light pulse and $\omega_L \pm \omega_{ba} \simeq \omega_L$. While strong stimulated Stokes-Raman scattering at ω_R was observed by us in several CdS samples, for production of maximum coherence in the spins it was advantageous to make use of two-wave mixing by introduction of an additional ω_R excitation present simultaneously in the 4905-Å dye laser along with ω_L.

The coherence or σ_T is examined by the intensity of Stokes and anti-Stokes coherent forward scattering from a probing 4880-Å argon laser beam. The conversion efficiency is given by[12]

$$\frac{P_s}{P_0} = \frac{1}{16}\left(\frac{d\sigma}{d\Omega}\right)_{4880\,\text{Å}} \frac{\lambda^2\eta^2L^2}{\epsilon} \sin^2\theta I, \quad (4)$$

where P_s is the sideband intensity and P_0 that of the 4880-Å probe. λ is the free space wavelength; ϵ, the dielectric constant; L, the sample thickness; and η, impurity concentration times the appropriate spin Boltzmann factor which is 0.45. The phase matching factor $I = 2(1 - \cos\Delta k\cdot L)/(\Delta k\cdot L)^2$, where $\Delta k = (k_L - k_R) - (k_L{}^P - k_R{}^P)$ and $k_L{}^P$ and $k_R{}^P$ are the wave vectors of the probe beam and its associated Raman sideband, respectively. In our case, I is of order unity.

The spin coherence is generated by a 5-ns dye-laser pulse of 100-W peak power operating simultaneously in two longitudinal modes ω_L and ω_R where $\omega_L - \omega_R = 32$ GHz. The spectral width of each mode is approximately 1.5 GHz. To achieve the sequence of pulses I and II shown in Fig. 1(b), the dye-laser output is split into two and then recombined collinearly after one of them is delayed by a time, τ, in an optical delay line.[2] A single-mode, cavity-dumped, 4880-Å argon laser provides a 100-mW peak power, 30-ns beam which can be electronically set to probe σ_T at any time, t, relative to the dye-laser pulse I [Fig. 1(c)]. The 4880- and 4905-Å beams are made collinear and focused by a 10-cm lens to a diameter of 100 μm. The sample is 0.5-mm thick and has an uncompensated donor concentration of $\sim 8 \times 10^{15}/\text{cm}^3$. It is cooled to 1.6 K; and an externally applied 12.75-kG magnetic field, perpendicular to $\hat{c}$, tunes the Zeeman splitting of the spins to be resonant with $\omega_L - \omega_R$. The probed signal (4880-Å Stokes line) is observed in the forward direction through a triple-pass Fabry-Perot interferometer in series with two 10-Å-bandwidth 4880-Å interference filters and detected with a phototube. The output of the phototube is fed into a boxcar followed by a multichannel analyzer for signal averaging.

For the observation of free induction, the argon probe was set coincident with either dye-laser pulses I or II [Figs. 1(b) and 1(c)]. The scattered Stokes and anti-Stokes intensities were of comparable magnitude and proportional to the probing 4880-Å beam intensity. In Fig. 2 we show the Stokes free-induction signal intensity as a function of the 4905-Å excitation intensity. It is seen that after a rapid initial increase, the signal saturates and at this point corresponds to about 10% conversion efficiency. The inset in Fig. 2 shows the temporal behavior of the free-induction decay observed with high-speed RCA 1P21 tube. The decay time is of the order of 3 ns which would correspond to an EPR linewidth of ~22 G.

In calculating θ from Eq. (3) (which applies only to an ideally coherent light pulse), modification is necessary in order to take account of the 1.5-GHz spectral width of the dye-laser pulse which is much larger than $1/\Delta t$. We only summarize the main results here. For small tipping angles, Eq. (3) is modified only to the extent that the effective intensity is reduced by a factor of 5. For large tipping angles, the analysis predicts that

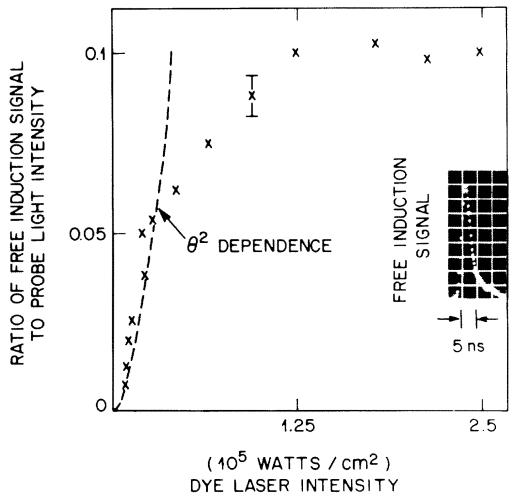

FIG. 2. Ratio of free induction signal to probing light intensity as a function of dye-laser intensity. Dashed curve indicates the initial θ^2 dependence.

the maximum average tipping angle is $\theta \sim \frac{1}{2}\pi$. Therefore, with $E_R \sim E_L$, the free-induction decay signal should initially be proportional to the square of the dye-laser intensity and saturate ($\theta = \frac{1}{2}\pi$) at 1.3×10^5 W/cm^2, taking $\Delta t = 5$ ns, $\epsilon = 9$, and $(d\sigma/d\Omega)_{4905} \sim 2\times10^{-19}$.[14] These predictions are in reasonable agreement with experimental results shown in Fig. 2. The maximum conversion efficiency calculated from Eq. (4) with $L = 0.05$ cm, $(d\sigma/d\Omega)_{4880} \sim 10^{-18}$ cm^2,[14] and $\eta = 8\times10^{15}\times0.45$, is 18%, taking into account a factor of 3 due to the Gaussian distribution of beam intensity. This is in good agreement with the experimental values of 10%, considering the factors-of-2 uncertainty in concentration, cross section, and imperfect phase matching.

We now turn our attention to the Raman echo. In addition to its dependence on τ which provides a direct measurement of the microscopic dephasing time, it also depends upon the strength of the excitation pulses and is given by the familiar expression[1,2]

$$\sigma_T^2(t = 2\tau) \propto \sin^2\theta_I \sin^4(\theta_{II}/2), \quad (5)$$

where θ_I, θ_{II} are the tipping angles produced by pulses I and II, respectively. The free-induction signals from either pulses I or II *alone* with the other cutoff are of the same magnitude and each corresponds to 10% sideband conversion of the probing beam. With both pulses applied and for an ideal sequence of $\pi/2$ pulses, the free-induction signal associated with pulse II should be zero[1] and the echo should be $\frac{1}{4}$ of the intensity of the free-induction signal from pulse I as seen from Eq. (5). While the observed free-induction signal associated with pulse II was not zero, it was nonetheless a factor of 10 smaller than that of pulse I as illustrated schematically in Fig. 1(d). The two dye-laser pulses and the echo signal for $\tau = 54$ ns (obtained with the center of the 30-ns-side 4880-Å probing beam set at $t = 2\tau$) are shown in Figs. 3(a) and 3(b), respectively. A very small amount of direct dye-laser fluorescence in the region of 4880 Å can still be observed which conveniently served as time markers. The rise and decay times shown in Figs. 3(a) and 3(b) are those of the high-gain RCA 8850 photomultiplier which, while slower than the RCA 1P21, has a higher sensitivity suitable for observing the echo. No echo was observed with either pulse I or II blocked as expected. Furthermore, we are able to set an upper limit of 1 part in 10^3 on any spurious reflection of the dye laser at $t = 2\tau$. The free-induction signal produced by such spurious reflections, if

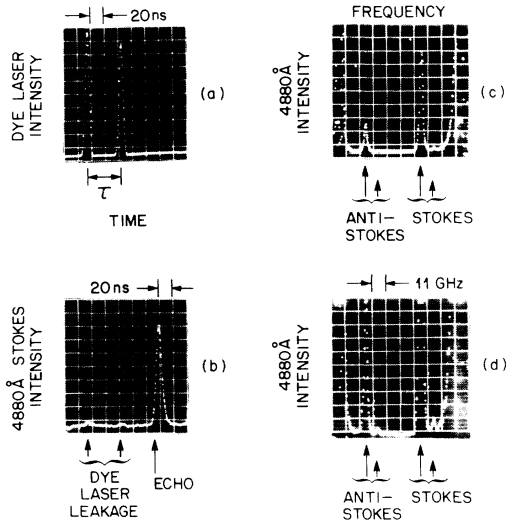

FIG. 3. (a) Dye-laser pulses separated by $\tau = 54$ ns. (b) Dye-laser leakage and the 4880-Å Stokes echo signal at $t = 2\tau$. (c) Frequency spectrum of probe and echo. The Stokes and anti-Stokes echoes are, respectively, from consecutive orders of the scanning Fabry-Perot (F-P) interferometer. These F-P orders are indicated by off scale laser probe appearing on each end of the figure. See text for explanation of doubling of Stokes and anti-Stokes. (d) Same as (c), except $5\times$ gain on vertical scale.

any, would be several orders of magnitude below the observed echo. The echo signal is a factor of 80 smaller than the free-induction signal associated with pulse I. This loss of a factor of 20 from the ideal case is likely due to either slight misalignment in optics or θ_{II} being somewhat less than $\pi/2$ (a factor of 2 off in θ_{II} reduces the echo signal by a factor of 50).

A Fabry-Perot interferometer scan of the frequency spectrum of the echo is shown in Figs. 3(c) and 3(d). In this particular instance there are two longitudinal modes in the 4880-Å probing light with a separation of 10 GHz and an intensity ratio of 40:1. As expected, the 4880-Å Stokes and anti-Stokes echo now also consists of two frequencies 10 GHz apart and with the same 40:1 intensity ratio. (The anti-Stokes line is weaker because of phase mismatching details.) This linearity again confirms that our probe beam intensity was always low enough to avoid stimulated emission. Echoes have been observed for τ up to 162 ns for this dilute sample (8×10^{15}/cm^3). No echo could be observed in a higher-concentration sample (7×10^{16}/cm^3), indicating rapid shortening of phase memory at higher concentration. Details of the phase memory measurements in CdS will be published later.

We wish to thank G. Devlin for his continual advice and assistance on many experimental details. We also thank R. Romestain for supplying us with the sample of CdS and many helpful discussions, along with S. McCall, L. R. Walker, and P. A. Wolff.

[1]E. L. Hahn, Phys. Rev. 80, 580 (1950). For detailed discussion see, for example, W. B. Mims, in *Electron Paramagnetic Resonance*, edited by S. Geschwind (Plenum, New York, 1972).

[2]N. A. Kurnit, I. D. Abella, and S. R. Hartmann, Phys. Rev. Lett. 13, 567 (1964). See also, for example, J. P. Gordon, C. H. Wang, C. K. N. Patel, R. E. Slusher, and W. J. Tomlinson, Phys. Rev. 179, 294 (1976).

[3]J. A. Giordmaine and W. Kaiser, Phys. Rev. 144, 676 (1966); for later references see A. Laubereau, G. Wochner, and W. Kaiser, Phys. Rev. A 13, 2212 (1976).

[4]S. R. Hartmann, IEEE J. Quantum Electron. 4, 802 (1968); R. Weingarten, Ph.D. thesis, Columbia University, 1972 (unpublished).

[5]See, for examples, Richard G. Brewer and E. L. Hahn, Phys. Rev. A 8, 464 (1973); M. M. T. Loy, Phys. Rev. Lett. 36, 1454 (1976); V. T. Nguyen, E. G. Burkhardt, and P. A. Wolff, Opt. Commun. 16, 145 (1976), and references therein.

[6]R. E. Slusher, C. K. N. Patel, and P. A. Fleury, Phys. Rev. Lett. 18, 77 (1967).

[7]C. K. N. Patel and E. D. Shaw, Phys. Rev. Lett. 24, 451 (1970); C. K. N. Patel, in *Laser Spectroscopy*, edited by R. G. Brewer and A. Mooradian (Plenum, New York, 1974).

[8]D. G. Thomas and J. J. Hopfield, Phys. Rev. 175, 1021 (1968).

[9]J. F. Scott, T. C. Damen, and P. A. Fleury, Phys. Rev. B 6, 3856 (1972).

[10]For a discussion of noncubic symmetry, see R. Romestain, S. Geschwind, and G. E. Devlin, Phys. Rev. Lett. 35, 803 (1975).

[11]Y. Yafet, Phys. Rev. 152, 858 (1966).

[12]R. Romestain, S. Geschwind, G. E. Devlin, and P. A. Wolff, Phys. Rev. Lett. 33, 10 (1974).

[13]Terrence L. Brown and P. A. Wolff, Phys. Rev. Lett. 29, 362 (1972); V. T. Nguyen and T. J. Bridges, Phys. Rev. Lett. 29, 359 (1972).

[14]Romestain, Geschwind, and Devlin, Ref. 10.

Trap-Controlled Dispersive Hopping Transport

G. Pfister, S. Grammatica, and J. Mort
Xerox Webster Research Center, Webster, New York 14580
(Received 16 August 1976)

The transition from transient trap-controlled hopping among traps has been observed in a polymer matrix doped with two transport molecules of different ionization potential. The nonequilibrium properties of the transport, characteristic of the disordered molecular state, are manifested by an apparent concentration-dependent trap depth.

The modulation of the microscopic charge transport through extended states by interaction with energetically shallow traps results in a trap-controlled drift mobility measured by the time-of-flight technique. A good example for an inorganic solid is the case of electron transport in CdS crystals.[1] This transport mechanism is characterized by the existence of thermal equilibrium in occupancy between extended states and shallow traps which is established in a time much shorter than the transit time t_T. Under these conditions the injected sheet of excess charge is said to move "coherently," since on the average the carriers experience the same large number of trapping events such that the relative dispersion of the propagating carrier sheet can be described with Gaussian statistics. Trap-controlled drift mobilities have also been measured in doped molecular crystals.[2] In this case, however, questions remain about the precise nature of the microscopic mobility in the ordered molecular state since the validity of a band picture is seriously in question.

Recent time-of-flight studies in molecularly doped polymers have provided firm evidence of an alternative microscopic mobility process. The ability to study charge transport as a function of the dopant molecule concentration allowed a clear identification of the mechanism as one involving the hopping of charge carriers within a random array of molecules.[3,4] This is consistent with the complete breakdown of a band picture in the disordered molecular state leaving hopping as the only possible process for the microscopic mobility in such systems. The dynamics of transient transport in disordered materials such as these are determined by stochastic processes and general agreement exists between experimental observation and recent theoretical work by Scher and Montroll.[5] The central point of this theory is

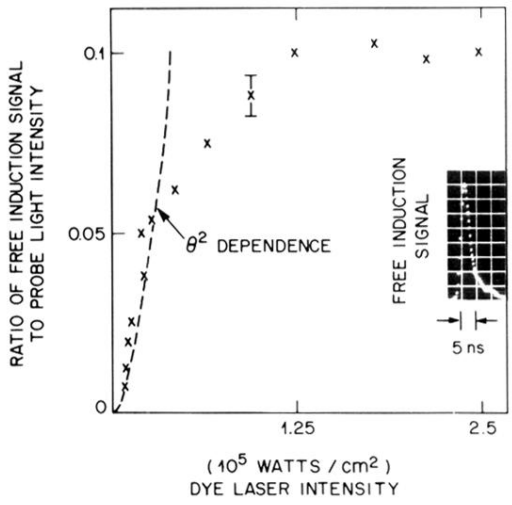

FIG. 2. Ratio of free induction signal to probing light intensity as a function of dye-laser intensity. Dashed curve indicates the initial θ^2 dependence.

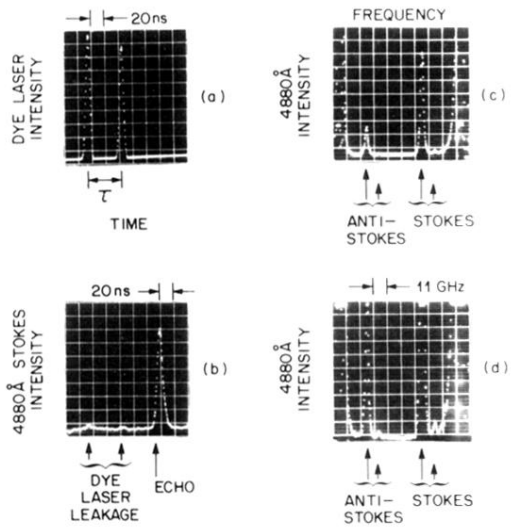

FIG. 3. (a) Dye-laser pulses separated by $\tau = 54$ ns. (b) Dye-laser leakage and the 4880-Å Stokes echo signal at $t = 2\tau$. (c) Frequency spectrum of probe and echo. The Stokes and anti-Stokes echoes are, respectively, from consecutive orders of the scanning Fabry-Perot (F-P) interferometer. These F-P orders are indicated by off scale laser probe appearing on each end of the figure. See text for explanation of doubling of Stokes and anti-Stokes. (d) Same as (c), except $5\times$ gain on vertical scale.